

# Shear-Induced Self-Assembly of Native Silk Proteins into Fibrils Studied by Atomic Force Microscopy

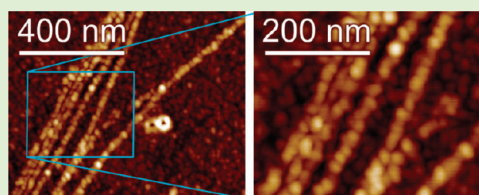
Imke Greving,<sup>†</sup> Minzhen Cai,<sup>‡</sup> Fritz Vollrath,<sup>†</sup> and Hannes C. Schniepp<sup>\*,‡</sup>

<sup>†</sup>Department of Zoology, University of Oxford, The Tinbergen Building, Oxford, OX1 3PS, United Kingdom

<sup>‡</sup>Applied Science Department, The College of William and Mary, Williamsburg, Virginia 23187, United States

## Supporting Information

**ABSTRACT:** Noncontact mode atomic force microscopy was used to investigate native silk proteins prepared in different ways. Low protein concentrations revealed that single protein molecules exhibit a simple, round shape with apparent diameters of 20–25 nm. Shearing the native protein solutions after extraction from the gland and prior to drying led to a beads-on-a-string assembly at the nanometer scale. Protein concentration had a significant effect on the morphology of the protein assemblies. At higher protein concentrations, shear-induced alignment into nanofibrils was observed, while lower concentrations lead to the formation of much thinner fibrils with a width of about 8 nm.



## INTRODUCTION

Silk is a natural high performance fiber featuring a rare combination of high strength and high breaking strain. Spun from a protein gel by insects and spiders at ambient temperatures and pressures, this biopolymer outperforms most manmade fibers.<sup>1,2</sup> It is generally believed that the outstanding toughness of silk is due to its sophisticated hierarchical structure involving amorphous and crystalline protein phases and their interplay.<sup>3–6</sup> The ability to artificially make silk with similarly good properties is a desirable goal given the many interesting engineering and biomedical applications of a wide range of natural silks.<sup>7,8</sup> Before synthetic high-performance silk fibers can be developed, however, several major challenges need to be overcome. For example, silk molecular and supramolecular structure needs to be better understood and so do the processes giving rise to the hierarchical assembly of the silk proteins into the final fiber.

Native high-molecular weight silk proteins are relatively difficult to handle. Accordingly, previous studies of silk proteins on a molecular level have mainly focused on regenerated or reconstituted silk (as well as recombinantly produced spider silk peptides) as these materials are more easily handled and prepared.<sup>6–14</sup> However, all of these artificially made silks have substantially different protein molecular weights<sup>15,16</sup> and, moreover, reconstituted and native silk dopes differ significantly in their rheological behavior.<sup>24</sup> Since artificial silks differ in both molecular-scale and macroscopic properties from natural silks it seems imperative to develop a rigorous understanding of the structure of native silk as well as its self-assembly behavior. In this work, we visualize native silk fibroin (SF) from the silk worm *Bombyx mori* at molecular resolutions using atomic force microscopy (AFM). Our results surpass previous studies in image resolution and provide new structural information about silk fibroin. Moreover, we use a sample preparation technique

that allows us to visualize the onset of shear-induced, molecular-scale self-assembly of native SF for the first time.

Silkworm silk fibroin consists of three proteins with different molecular weights ( $M_w$ ): heavy chain fibroin (350 kDa), light chain fibroin (25 kDa), and so-called P25 (30 kDa); these proteins occur in the mass ratios 6:6:1.<sup>17</sup> Concerning the spatial conformation of native SF molecules there is hardly any data in the literature. The most relevant work we found in this respect is a single-molecule AFM study of native *Bombyx mori* SF by Inoue et al. who suggest a rod-like shape for SF,<sup>18</sup> which was also suggested by Viney et al. from birefringence.<sup>19</sup> However, the model that Inoue et al. developed is based on contact-mode AFM images that were acquired in air, where tip–sample interactions lead to significant lateral forces<sup>20</sup> that are strong enough to frequently displace, deform, and disrupt biomolecules.<sup>21</sup> We believe that the data reported by Inoue et al. is significantly distorted through limitations of their imaging approach. Our data, collected with a much gentler imaging technique, suggests that their model needs to be corrected.

For artificial silks, there is structural protein data available; however, the results from different research groups diverge significantly. Two different types of shapes have been suggested for silk proteins: rod-like<sup>22</sup> and micellar/globular.<sup>12,23</sup> Moreover, there is a substantial spread in the reported protein sizes, ranging from a few to several hundred nanometers. This is in line with the observed differences in molecular weight,<sup>14–16</sup> which are due to variations in the preparation methods for these artificial silks between research groups, using different chaotropic agents and so on.<sup>15,16,23,24</sup> This uncertainty and spread associated with artificial silk in terms of protein mass

Received: October 26, 2011

Revised: December 24, 2011

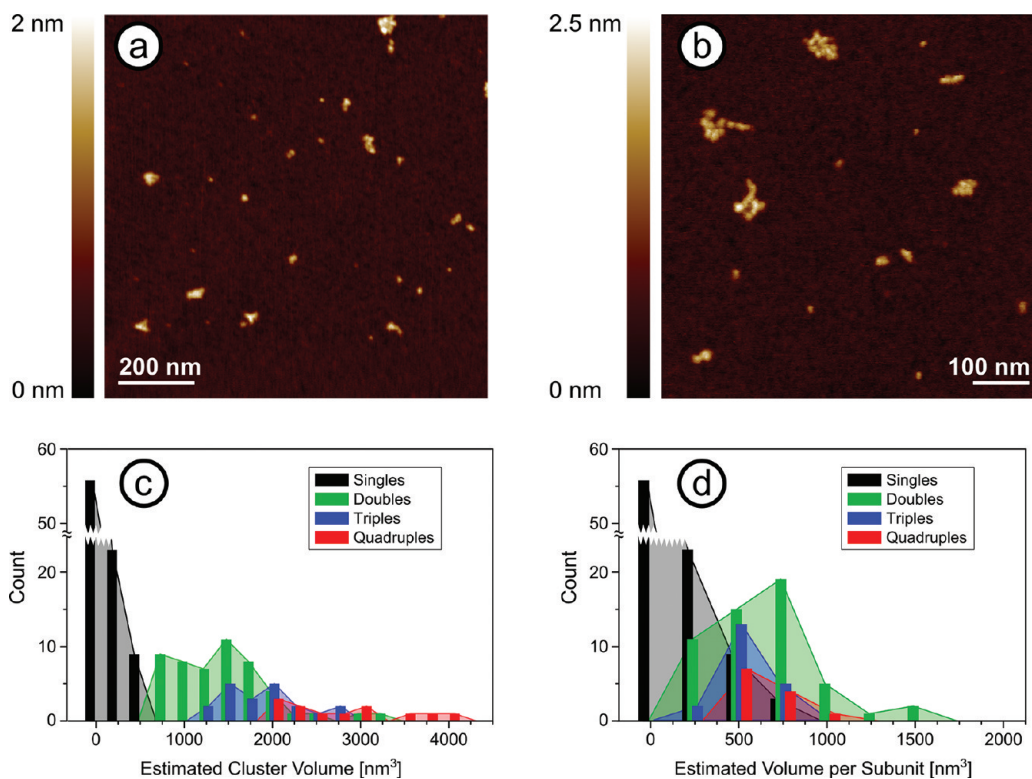


**Figure 1.** (a, b) Noncontact AFM topography images from native silk molecules (SF) deposited on a cleaved mica surface from a 1:1000 diluted solution without shear. The smaller features are round, have a diameter of 20–25 nm, a height of about 1.2 nm, and are most likely individual silk proteins. The larger objects are clusters of several proteins. (c) Histograms showing the volumes of proteins and protein clusters determined from AFM topography data. (d) Same as (c), except that volumes were divided by the number of apparent subunit within each cluster.

and shape highlights the importance of studying native silk protein.

In the hierarchical structure of the silk fiber, highly repetitive amino acids of the silk proteins are assembled into  $\beta$ -sheets and  $\alpha$ -helical structures characterized, for example, by NMR or X-ray scattering.<sup>1,4,25</sup> In addition, AFM and electron microscopy provides evidence for larger structural building blocks of the fiber, so-called nanofibrils with diameters in the range 20–170 nm.<sup>26–28</sup> Some authors have suggested that such nanofibrils are actually bundles of even smaller nanofibrils with diameters of 5 nm<sup>29</sup> or with diameters of 10–15 nm.<sup>3</sup> However, there is no direct experimental evidence supporting the existence of these 5–15 nm diameter nanofibrils. While the hierarchical structure of the silk fiber is known to some extent, any details about its assembly from the silk dope are still unknown. Starting at the level of individual, aqueously dissolved protein molecules, this multiscale process is extremely challenging to study experimentally. Known contributing factors in this process are pH changes along with a shift in ion concentration,<sup>30,31</sup> which is accompanied by shear and flow-elongation (prealigning the protein molecules prior to fiber formation<sup>32</sup>).

Our experimental approach is based on high-resolution AFM imaging of dry samples made from an aqueous solution of native SF. We employ the nondestructive noncontact mode, where the AFM probe is guided across the surface sensing attractive van der Waals forces<sup>33</sup> so that the tip rarely touches the sample and interactions between tip and sample are minimized. In some of our samples, we sheared the aqueous protein solution during the drying process using a spin coater. These shear-dried samples, thus, represent a snapshot of the structural response of silk protein solution to shear, which is

then revealed via AFM imaging with nanometer resolutions. While spin coating has been used with reconstituted or recombinant silk before,<sup>34,35</sup> our work is the first report of application of such a procedure with native silk proteins. Overall, our experiments provide novel insights into the protein shape of native SF molecules, as well as a first direct evidence for their molecular-scale self-assembly behavior under shear conditions.

## EXPERIMENTAL SECTION

**Sample Preparation.** Native silk protein from glands of 18 *Bombyx mori* silk worms (5th instar) were washed in deionized water to remove the sericin coating. Then, the gel like silk was left to homogenize overnight at 6 °C in deionized water to obtain a stock solution of native silk fibroin (SF).<sup>15</sup> For AFM sample preparation, six of the obtained SF stock solutions with a concentration of  $10 \pm 0.5$  mg/mL were diluted by a factor of 1:10, 1:100, and 1:1000 using picopure water (Synergy Millipore, Billerica, MA; resistivity 18 M $\Omega$ -cm at 25 °C).

For high-resolution AFM imaging, all samples were prepared using freshly cleaved, atomically smooth mica sheets as substrates. The protein was deposited on the substrates from the diluted aqueous solutions in two distinct ways. In the first way (“sheared samples”), a shear flow was created in the SF of three different stock solutions by spin-coating a 200  $\mu$ m droplet on the substrate at 2000 rpm using a WS-650SZ Spin Processor (Laurell Technologies Corporation, North Wales, PA). After 2 min, the samples were dry and ready for AFM examination; four different sheared samples were imaged. In the second way of preparing the samples great care was taken to avoid any shearing of the solution (“non-sheared samples”). A droplet was therefore placed on the mica surface and kept under humid atmosphere for 30 min. Afterward, the mica was gently flushed with deionized water and dried with nitrogen gas (Nitrogen 5.0, GTS

Welco, Allentown, Pennsylvania). In total, six different stock solutions were used to prepare the “non-sheared” samples, and nine samples of different dilutions were imaged. In all of these images we observed a bead-like structure with comparable sizes.

**Atomic Force Microscopy.** AFM measurements were conducted at room temperature using a NTEGRA Prima Scanning Probe Laboratory (NT-MDT, Zelenograd, Russia). In order to minimize tip–sample interactions and deformations of the soft protein molecules, scanning was carried out in true noncontact mode.<sup>33</sup> The AFM probes were ACTA silicon cantilevers (APPNANO, Santa Clara, California) with a typical resonance frequency of  $f = 300$  kHz, a radius of curvature of  $r < 10$  nm, and a spring constant of  $k = 40$  N/m. To get AFM images with highest resolution, ultrasharp tips with a radius of curvature  $r < 5$  nm were used (APPNANO, ACTA-SS silicon cantilevers,  $f = 300$  kHz,  $k = 40$  N/m). The high-resolution images were obtained using tip vibration amplitudes of less than 50 nm.

For quantitative characterization of adsorbed proteins via AFM it is important to know that there is an asymmetry between lateral (“ $x/y$ ”, in the substrate plane) and vertical (“ $z$ ”, normal to the substrate plane). In the vertical direction, biomolecules usually appear smaller than expected due to a combination of several phenomena: (i) protein deformation due to attractive forces between the substrate and the proteins,<sup>36,37</sup> (ii) protein dehydration,<sup>33,38</sup> (iii) vertical forces between tip and sample that can lead to deformations during imaging,<sup>33</sup> (iv) spatial variations of the tip–sample interactions leading to modulations of the tip–sample gap,<sup>33,39</sup> and (v) averaging of the tip–sample interactions over an effective interaction area larger than the imaged features.<sup>36</sup> In the lateral direction, in contrast, biomolecules often appear wider than expected due to the finite width of the AFM probe leading to a broadening through convolution and because the attractive interactions with the substrate<sup>36</sup> lead to flattening of soft molecules. These uncertainties in the assessment of the precise lateral and vertical dimensions of small objects via AFM become substantial when their size approaches the size of the AFM probe, such as in the case of individual protein molecules.

## RESULTS

Noncontact mode AFM images of a nonsheared sample prepared from a 1:1000 diluted silk solution are shown in Figure 1a,b. The images show small, isolated objects of different sizes. The smallest objects are most likely individual silk fibroin molecules and have a round shape of 20–25 nm diameter, determined as the full width at half-maximum (fwhm) of topography cross sections; the corresponding heights above background are about 1.2 nm. The larger objects feature more irregular shapes with the higher-magnification scan (Figure 1b) showing the larger objects to be clusters of several of the smaller, round objects, each most likely representing one heavy chain fibroin. We carried out a statistical analysis of the volumes of these objects, taking into account 91 single objects, as well as 85 clusters consisting of 2–4 subunits. Figure 1c shows a histogram with the volumes of each of these objects. As expected, the measured volumes increase with the number of subunits in each cluster. For Figure 1d, the volumes of clusters were divided by the number of apparent subunits in each cluster. Objects consisting of only one subunit (“singles”, data in black), feature an asymmetric histogram dominated by small particles with volumes of less than 250 nm<sup>3</sup>. Clusters consisting of 2–4 subunits feature roughly symmetric volume distributions centered around 750 nm<sup>3</sup>. In addition, we followed an alternate method proposed by Pietrasanta et al. to determine the protein volumes based on our AFM topography,<sup>40</sup> by which we obtained a much smaller value of about 315 nm<sup>3</sup>; more details of this procedure are provided in the Supporting Information.

To compare our AFM results with volume estimates of single proteins based on their molecular weight we use the formula  $V = \nu \times M_w / N_A$ , where  $M_w$  is the molecular weight,  $N_A$  is Avogadro’s number, and  $\nu = 0.725$  cm<sup>3</sup>/g is the partial molar volume for fibroin.<sup>41,42</sup> For the known molecular weight of the heavy chain silk fibroin, 350 kDa, this leads to a volume of  $V = 415$  nm<sup>3</sup>; for a heavy chain linked by a disulfide bond to a light chain, 375 kDa, this leads to a volume of  $V = 451$  nm<sup>3</sup>. Due to the inaccuracies in the AFM measurements of protein volumes a 1:1 correspondence between the measured values (315–750 nm<sup>3</sup>) and predicted numbers (415–450 nm<sup>3</sup>) cannot be established with certainty. Nevertheless, we suggest the following interpretation of our AFM data. The larger ones of the single-unit, round objects are individual heavy chains; the smaller single-unit objects are light-chain and P25 fibroin. In the clusters, each of the apparent subunits corresponds to one heavy chain. Light chains and P25 fibroins may be mixed in, although not recognizable as distinct topography features. In order to improve the lateral accuracy of AFM estimates, it would be necessary to determine the size and shape of each of the used AFM tips.<sup>43</sup> To reduce the significant uncertainty in the protein heights determined via dynamic-mode AFM a rigorous understanding of the effective tip–sample potential is needed, which is still an area of active research.<sup>36</sup>

When we increased the protein concentration to the 1:10 level we found a fully covered surface; the corresponding AFM images are shown in Figure 2 at two different magnification

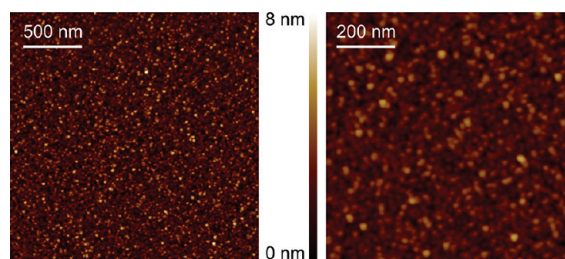


**Figure 2.** Noncontact mode AFM topography images of silk protein prepared under low-shear conditions on a mica substrate from a 1:10 diluted aqueous protein solution.

levels. We observe a complete, homogeneous and isotropic coverage of small objects on the surface. Although more difficult to determine due to the surface roughness, many of these objects feature diameters in the 20–25 nm range and are, thus, likely to correspond to individual heavy chain proteins in analogy to our interpretation of Figure 1. There is no manifest symmetry, anisotropy, positional, or directional correlation or organized structure of any kind. The protein positions and directions are completely random, uncorrelated, and not organized. The same is true for the organization of the individual proteins in the reported clusters observed at the lower 1:1000 concentration; no apparent organization into structure above the single-molecule level, other than the “condensation” into clusters itself.

In contrast to our observations on the unsheared solutions, we found significant and intriguing molecular self-organization of the silk proteins when the silk solutions were exposed to shear during the deposition onto the mica substrates. Proteins that were deposited under shear from the 1:10 solution are featured in Figure 3, which shows a series of noncontact mode AFM images at different magnifications. Figure 3a features bright, diagonal lines on a dark background. In terms of size,

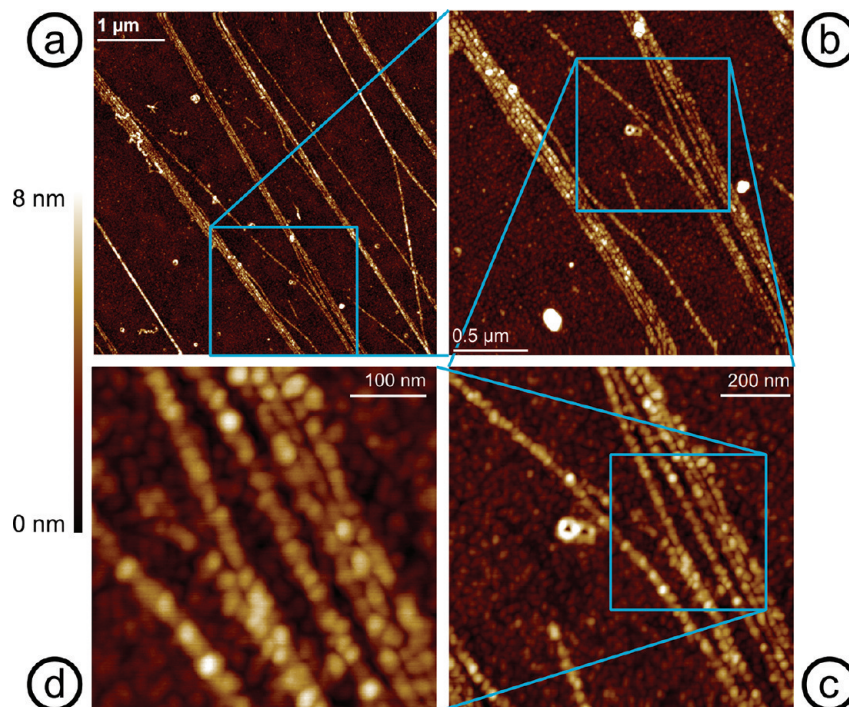


**Figure 3.** Noncontact mode AFM topography images showing a sample that was prepared by spin-coating a 1:10 silk solution. The images show self-assembly of silk protein into linear, thread-like structures.

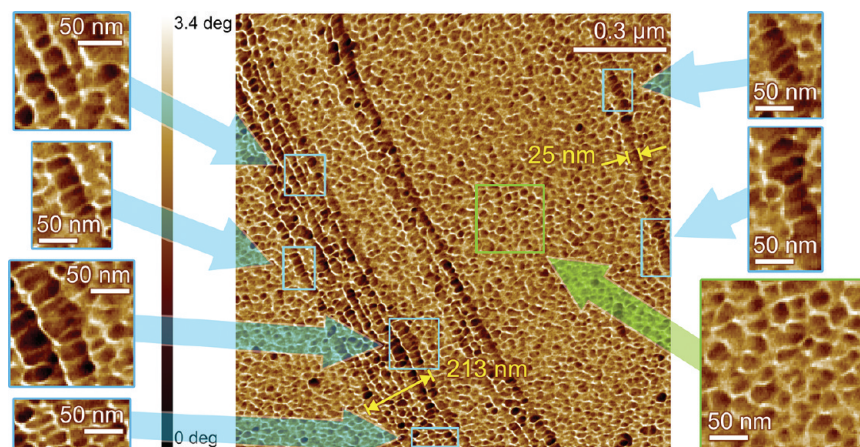


**Figure 4.** Noncontact AFM phase image of the same sample shown in Figure 3. Areas in colored boxes are featured with higher magnification on the left and right sides of the main image. The majority of the sample looks like the area highlighted in the green box: unorganized, round protein molecules. The blue boxes highlight areas in the nanofibrils featuring anisotropic conformation of the proteins. Sections across a single nanofibril and a bundle of nine nanofibrils are indicated in yellow.

shape, distribution, and density of the proteins, the structure in the dark areas of Figure 3 looks very similar to Figure 2, that is, the image of a sample made from the same silk solution *without* shear. We, thus, assume that the dark areas of Figure 3 represent homogeneously distributed, randomly positioned protein molecules (or small agglomerates thereof). In contrast, the bright, diagonal lines represent elevated structures on the surface protruding from the “amorphous” background of randomly placed proteins by about 2–4 nm. These lines have varying widths, ranging from 25–250 nm, and they are branching and forking in several areas. They are predominantly orientated in radial direction, normal to the spinning axis of the sample (see Supporting Information).

The higher-magnification image in Figure 3b shows that each of the lines consists of a discrete number of constituent

nanofibrils. Figure 3c reveals that each of these nanofibrils consists of a discrete series of elements, exhibiting a “beads on a string” type of morphology. Based on their diameters, 20–25 nm, each of these “beads” is probably a single silk protein. The morphology and organization of each of the beads is not highly uniform; as can be seen in Figure 3c,d they vary in height (indicated by differences in color) and in diameter. The beads are not lined up perfectly within each of the nanofibrils; their position is laterally offset by up to 10 nm within the nanofibril (see Figure 3d). A phase image corresponding to the noncontact mode topography images in Figure 3 is shown in Figure 4. The diameter of an individual nanofibril was determined from this phase image to be about 25 nm. We also determined the width of a bundle consisting of nine nanofibrils shown in Figure 4. Assuming close packing of the

fibrils in the bundle we can determine the diameter of a single fibril with higher precision, since the error due to the finite diameter of the probe (5–10 nm) is distributed over the entire bundle (213 nm) and, thus, negligible. The obtained value  $213 \text{ nm} \div 9 \approx 23.7 \text{ nm}$  is close to the 25 nm obtained for a single fibril, which suggests that size overestimation due to probe diameter can be neglected even for single-bundle measurements in this case.

We further investigated the length of protein molecules along the direction of the nanofibrils. Four topography cross sections in the center of the nanofibrils, following the fibril direction, were generated from AFM imaging data. Fourier transforms of these cross sections were carried out and the frequency peak corresponding to the protein periodicity was identified. The corresponding periodicities were 17.52, 16.63, 17.20, and 15.32 nm, leading to an average of  $16.7 \pm 1.0 \text{ nm}$ . The length of the proteins along the fibers,  $\approx 17 \text{ nm}$ , is thus significantly smaller than the observed width of the proteins perpendicular to the fibril axis,  $\approx 24 \text{ nm}$ . In some areas, highlighted by blue boxes in Figure 4, this shape anisotropy of the beads in the fibers is obvious. In contrast, all the proteins between the fibrils (a representative area is highlighted in the green box) are randomly distributed and round (isotropic) with similar diameters, comparable to the film-like structures observed without shear.

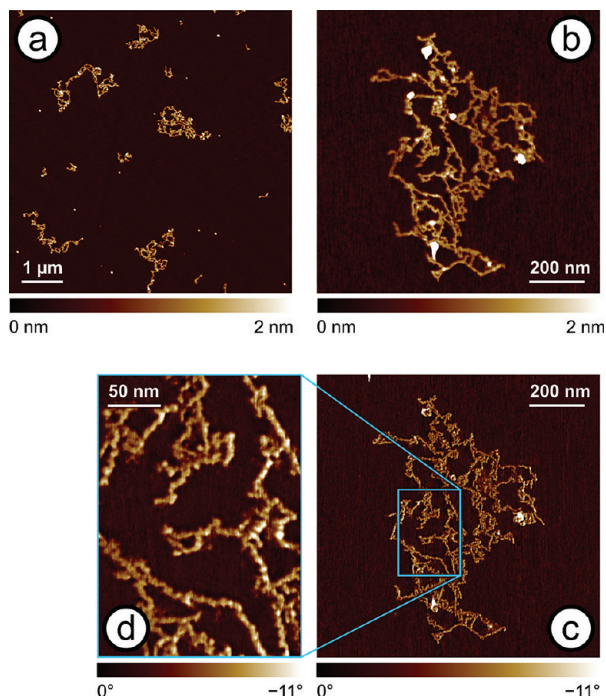


**Figure 5.** Noncontact AFM images of silk deposited from an aqueous 1:1000 solution by spin-coating, which induced shear in the solution: (a, b) topography image; (c, d) phase images. The proteins self-assemble into nanofibrils. The diameter is less than one of the globular single proteins shown in Figure 1, which were deposited from the same solution. This indicates that the protein undergoes conformational changes during the spin-coating process.

When proteins from a 1:1000 silk solution are deposited on mica under shear, we observe yet another mode of protein self-organization on the substrate, shown in Figure 5. Prepared under these conditions the great majority of the protein on the surface is organized into sparsely distributed, large assemblies.

Figure 5a shows a noncontact mode AFM topography image featuring several of these assemblies of different size; in total, we imaged 50 of these structures. Figure 5b,c show a topography image at higher magnification and its corresponding phase image, respectively. Figure 5d shows a phase image at a yet higher magnification. The structures appear like random coils formed out of one or several threads (“nano-fibrils”), similar to what is known from other 1D macromolecules, such as DNA<sup>44</sup> or synthetic polymers.<sup>45</sup>

The string-like, 1D morphology of these assemblies suggests that they were not formed on the surface but in solution upon application of shear. The high-resolution AFM image in Figure 5 (right panel) reveals that these nanofibrils have a diameter on the order of 8 nm and an apparent height of about 0.6 nm. Like other AFM data of proteins, the diameter is most likely overestimated, whereas the height is an underestimate. We also noticed a periodic structure along the direction of the nanofibrils, hinting at the next smaller level of structural organization. Eight short topography cross sections, 2–5 periods long, were taken, and the average period was determined to be  $8.6 \pm 1.2 \text{ nm}$ .

## DISCUSSION

A comparison between the results for sheared and unsheared samples revealed several fundamental differences. In the unsheared samples the protein was randomly distributed on the substrate. At the lower, 1:1000 concentration, we observed individual protein molecules of globular shape on the surface, along with clusters that most likely formed on the substrate upon adsorption. This suggests that there is no notable protein aggregation in the solution under these conditions. We determined the lateral dimensions of the protein, 20–25 nm, and its apparent height on the substrate, 1.2 nm. These findings are in clear contrast to the only other AFM work on native silk proteins in the literature by Inoue et al.,<sup>18</sup> who found rod-like structures of 60 nm length under similar conditions. The discrepancy can be easily explained by the fact that Inoue et al. used contact-mode AFM, which is known to disrupt, displace, and distort biomolecules during imaging. Our data taken in noncontact mode thus represents protein structure without comparable artifacts. Furthermore, the resolution of the images in the work of Inoue et al. is low compared to the AFM images presented here.

At the higher 1:10 concentration we observe a completely covered substrate, where the proteins are packed more densely. This close-packed morphology does not allow measuring the protein diameter with high precision or the protein height. However, given the similar shape and comparable diameter, we suspect that the protein molecules feature the same conformation in both cases, just at different packing densities. Importantly we did not observe any spontaneous fibrillation or elongation of the globular shapes upon increasing the protein concentration as reported in Inoue’s work<sup>18</sup> as well as in studies on recombinant spider silks<sup>12</sup> and reconstituted silks.<sup>23,48</sup> As we have shown, however, exposing silk solutions to shear can trigger such transformations quite easily, so it is possible that these authors have accidentally sheared their samples to a small degree during normal sample handling, for instance, while pipetting the solutions.

When we sheared the protein solutions, we found two interesting modes of protein organization depending on the concentration. At the higher 1:10 concentration, part of the protein on the surface is organized into nanofibrils (and

branching bundles thereof) that run on the substrate surface almost straight. The size of the smallest visible building blocks in these nanofibrils is similar to the dimensions of the single protein molecules and film-like structures observed without shear. Hence, these nanofibrils observed here are likely to be shear aligned single protein molecules. It would be very interesting to know whether these 25 nm wide nanofibrils are related to the recently observed 20 nm wide fibrils in cross sections of *Bombyx mori* fibers<sup>28</sup> or to the 90–170 nm wide nanofibrils reported elsewhere in the literature.<sup>26,27</sup>

At the lower 1:1000 concentration, we observed that the protein on the surface had the shape of thin strings with a diameter of about 8 nm that are randomly coiled. Their diameter is thus significantly smaller than any of the other structures obtained in this work. All the other structures featured in Figures 1–4 have building blocks with lateral dimensions in the range of 17–25 nm. This includes the single molecules (and clusters thereof) featured in Figure 1, the homogeneously distributed, close-packed proteins in Figures 2–4, and the proteins forming the nanofibrils in Figures 3 and 4. Therefore, the nanofibrils observed in Figure 5 cannot simply be a chain of the proteins observed in the other figures; instead, the protein must have undergone a transformation into a thinner and longer conformation upon assembly into the nanofibrillar morphology. The diameter of these nanofibrils,  $\approx 8$  nm, is close to what Hakimi et al.<sup>29</sup> (5 nm) or Zhao et al.<sup>3</sup> (10–15 nm) have proposed. However, both groups did not present experimental evidence for the existence of such small nanofibrils. The periodicity observed along these thin nanofibrils,  $8.6 \pm 1.2$  nm, is much shorter than the dimensions of individual proteins and is thus likely to represent an intramolecular structure of the proteins in the elongated conformation. In the absence of any other experimental evidence on the nanofibrils in the literature, however, further conclusions cannot be drawn at this point. It is worth noting that structural elements of similar size have been detected for spider silk by Grubb and Jelinski, who have found 7 nm as a lower limit for the length of  $\beta$ -sheet crystals along the fiber axis;<sup>46</sup> other authors report an average fibril periodicity of 7 nm from small-angle X-ray scattering.<sup>47</sup>

The mechanism for both forms of assembly is currently unknown. The straighter, thicker nanofibrils from the 1:10 concentration may, for instance, be formed through attractive interactions between single proteins. In that case, attractive forces between proteins may deform the protein molecules and thus account for the observed anisotropy. For the lower 1:1000 concentration we hypothesize that the conformational change might have been possible due to unfolding of the silk protein (loss in structure) at low concentrations, also observed in solution scattering on native silk,<sup>15</sup> which allowed an aggregation into thin fibrils. Further investigation will also be needed to determine the influence of the substrate on the formation of the reported structures. All experiments here were carried out using mica, which is a strongly hydrophilic, high-energy surface with a significant negative surface charge under these conditions. It will be interesting to see if the same structures can be observed on a low-energy, hydrophobic surface.

## CONCLUSIONS

Native silk proteins, obtained from silkworm glands, were diluted with picopure water to different concentrations and deposited on mica substrates with and without shearing the

solution. The samples were investigated by noncontact mode AFM for structural analysis of the obtained protein structures. Deposition of low protein concentrations onto a mica substrate yielded samples featuring single protein molecules and small agglomerates thereof, with random organization. The single molecules featured appear to be of globular shape with diameters in the range 20–25 nm and an apparent height of  $\approx 1.2$  nm, which is in clear contrast to the observed rod-like structures by Inoue et al.<sup>18</sup> At an increased concentration we found that the substrate was completely covered with objects of similar size and shape in random and uncorrelated positions and orientations. We did not observe spontaneous fibrillation at higher protein concentrations as reported previously in recombinant spider silks and reconstituted silkworm silk.<sup>12,48</sup> When shear was applied during deposition by spin-coating the silk protein solution onto the substrates, we obtained fibrillar structures of two different kinds, depending on the concentration. At high (1:10) protein concentrations we found single molecules that are shear aligned into threadlike structures and bundles thereof. The average sizes of the aligned molecules are comparable to the single molecule diameters, albeit slightly compressed in the direction parallel to the fibrils, and suggest a prefibrillar state. The average width of 25 nm is close to the 20 nm observed for nano fibrils in *Bombyx mori* fibres.<sup>28</sup> At low (1:1000) concentration of the silk proteins we found randomly coiled nanofibrils of much thinner diameter,  $\approx 8$  nm. To organize into this structure, the protein has to undergo a significant conformational transformation, as the protein exhibits a significantly larger diameter in single-molecule conformation. We hypothesize that the observed conformational change was possible due to an unfolding of the protein at low concentrations<sup>15</sup> and led to an aggregation into thin fibrils.

## ASSOCIATED CONTENT

### Supporting Information

More details on the statistical analysis of AFM protein data and the orientation of the fibrils with respect to the spinning axis. This material is available free of charge via the Internet at <http://pubs.acs.org>.

## AUTHOR INFORMATION

### Corresponding Author

\*E-mail: [schniepp@wm.edu](mailto:schniepp@wm.edu). Phone: 757-221-2559. Fax: 757-221-2050.

## ACKNOWLEDGMENTS

H.C.S. acknowledges support through the Thomas F. Jeffress and Kate Miller Jeffress Memorial Trust, under Grant No. J-1012. I.G. acknowledges studentship and research funding from EPSRC and F.V. acknowledges support through AFOSR (FA9550-09-1-0111) and ERC (SP2-GA-2008-233409). The authors thank Dr. A. Terry for help with the manuscript.

## REFERENCES

- (1) Porter, D.; Vollrath, F. *Adv. Mater.* **2009**, *21*, 487–492.
- (2) Vollrath, F.; Knight, D. P. *Nature* **2001**, *410*, 541–548.
- (3) Zhao, C.; Asakura, T. *Prog. Nucl. Magn. Reson. Spectrosc.* **2001**, *39*, 301–352.
- (4) Riek, C.; Vollrath, F. *Int. J. Biol. Macromol.* **2001**, *29*, 203–210.
- (5) Krasnov, I.; Diddens, I.; Hauptmann, N.; Helms, G.; Ogureck, M.; Seydel, T.; Funari, S. S.; Müller, M. *Phys. Rev. Lett.* **2008**, *100*, 048104.

- (6) Oroudjev, E.; Hayashi, C.; Soares, J.; Arcidiacono, S.; Fossey, S. A.; Hansma, H. G. *Mater. Res. Soc. Symp. Proc.* **2003**, 738, G10.4.1–7.
- (7) Hakimi, O.; Kaplan, D. P.; Vollrath, F.; Vadgama, P. *Composites B* **2007**, 38, 324–337.
- (8) Huang, W.; Begum, R.; Barber, T.; Ibba, V.; Tee, N. C. H.; Hussain, M.; Arastoo, M.; Yang, Q.; Robson, L. G.; Lesage, S.; Gheysens, T.; Skaer, N. J. V.; Knight, D. P.; Priestley, J. V. *Biomaterials* **2012**, 33, 59–71.
- (9) Yamada, K.; Tsuboi, Y.; Itaya, A. *Thin Solid Films* **2003**, 440, 208–216.
- (10) Pirzer, T.; Geisler, M.; Scheibel, T.; Hugel, T. *Phys. Biol.* **2009**, 6, 025004.
- (11) Rammensee, S.; Huemmerich, D.; Hermanson, K.; Scheibel, T.; Bausch, A. *Appl. Phys. A: Mater. Sci. Process.* **2006**, 82, 261–264.
- (12) Oroudjev, E.; Soares, J.; Arcidiacono, S.; Thompson, J.; Fossey, S.; Hansma, H. G. *Proc. Natl. Acad. Sci. U.S.A.* **2002**, 99, 6460–6465.
- (13) Geisler, M.; Pirzer, T.; Ackerschott, C.; Lud, S.; Garrido, J.; Scheibel, T.; Hugel, T. *Langmuir* **2008**, 24, 1350–1355.
- (14) Krishnaji, S. T.; Huang, W.; Rabotyagova, O.; Kharlampieva, E.; Choi, I.; Tsukruk, V. V.; Naik, R.; Cebe, P.; Kaplan, D. L. *Langmuir* **2011**, 27, 1000–1008.
- (15) Greving, I.; Dicko, C.; Terry, A.; Callow, P.; Vollrath, F. *Soft Matter* **2010**, 6, 4389–4395.
- (16) Yamada, H.; Nakao, H.; Takasu, Y.; Tsubouchi, K. *Mater. Sci. Eng., C* **2001**, 14, 41–46.
- (17) Inoue, S.; Tanaka, K.; Arisaka, F.; Kimura, S.; Ohtomo, K.; Mizuno, S. *J. Biol. Chem.* **2000**, 275, 40517–40528.
- (18) Inoue, S.; Magoshi, J.; Tanaka, T.; Magoshi, Y.; Becker, M. J. *Polym. Sci., Part B* **2000**, 38, 1436–1439.
- (19) Viney, C. *Supramol. Sci.* **1997**, 4, 75–81.
- (20) Zhong, Q.; Inniss, D.; Kjoller, K.; Elings, V. B. *Surf. Sci. Lett.* **1993**, 290, L688–L692.
- (21) Bezanilla, M.; Drake, B.; Nudler, E.; Kashlev, M.; Hansma, P. K.; Hansma, H. G. *Biophys. J.* **1994**, 67, 2454–2459.
- (22) Huang, T.; Ren, P.; Huo, B. *J. Appl. Polym. Sci.* **2007**, 106, 4045–4059.
- (23) Jin, H.; Kaplan, D. *Nature* **2003**, 424, 1057–1061.
- (24) Holland, C.; Terry, A. E.; Porter, D.; Vollrath, F. *Polymer* **2007**, 48, 3388–3392.
- (25) Termonia, Y. *Macromolecules* **1994**, 27, 7378–7381.
- (26) Poza, P.; Pérez-Rigueiro, J.; Elices, M.; Lorca, L. J. *Eng. Fract. Mech.* **2002**, 69, 1035–1048.
- (27) Putthanarat, S.; Stribeck, N.; Fossey, S. A.; Eby, R. K.; Adams, W. W. *Polymer* **2000**, 41, 7735–7747.
- (28) Du, N.; Yang, Z.; Liu, X. Y.; Li, Y.; Xu, H. Y. *Adv. Funct. Mater.* **2011**, 21, 772–778.
- (29) Hakimi, O.; Knight, D. P.; Vollrath, F.; Vadgama, P. *Composites B* **2007**, 38, 324–337.
- (30) Dicko, C.; Kenney, J.; Knight, D.; Vollrath, F. *Biochemistry* **2004**, 43, 14080–14087.
- (31) Dicko, C.; Kenney, J. M.; Vollrath, F. *Adv. Protein Chem.* **2006**, 73, 17–53.
- (32) Knight, D. P.; Vollrath, F. *Philos. Trans. R. Soc. London, Ser. B* **2002**, 357, 155–163.
- (33) Garcia, R.; Perez, R. *Surf. Sci. Rep.* **2002**, 47, 197–301.
- (34) Junghans, F.; Morawietz, M.; Conrad, U.; Scheibel, T.; Heilmann, A.; Spohn, U. *Appl. Phys. A: Mater. Sci. Process.* **2006**, 82, 253–260.
- (35) Jiang, C.; Wang, X.; Gunawidjaja, R.; Lin, Y.-H.; Gupta, M. K.; Kaplan, D. L.; Naik, R. R.; Tsukruk, V. V. *Adv. Funct. Mater.* **2007**, 17, 2229–2237.
- (36) Santos, S.; Barcons, V.; Christenson, H. K.; Font, J.; Thomson, N. H. *PLoS ONE* **2011**, 6, e23821.
- (37) Pietrasanta, L. I.; Schaper, A.; Jovin, T. M. *Nucleic Acids Res.* **1994**, 22, 3288–3292.
- (38) van Hulst, N. F.; Garcia-Parajo, M.; Moers, M. F.; Veerman, M. H. P.; Ruiters, A. G. T. *J. Struct. Biol.* **1997**, 119, 222–231.
- (39) van Noort, S. J. T.; van der Werf, K. O.; de Groot, B. G.; van Hulst, N. F.; Greve, J. *Ultramicroscopy* **1997**, 69, 117–127.
- (40) Pietrasanta, L. I.; Thrower, D.; Hsieh, W.; Rao, S.; Stemmann, O.; Lechner, J.; Carbon, J.; Hansma, H. *Proc. Natl. Acad. Sci. U.S.A.* **1999**, 96, 3757–3762.
- (41) Fischer, H.; Polikarpov, I.; Craievich, A. F. *Protein Sci.* **2004**, 47, 2825–2828.
- (42) Zhao, H. P.; Feng, X. Q.; Shi, H. J. *Mater. Sci. Eng. C* **2007**, 27, 675–683.
- (43) McConney, M. E.; Singamaneni, S.; Tsukruk, V. V. *Polym. Rev.* **2010**, 50, 235–286.
- (44) Hansma, H. G.; Vesenka, J.; Siegerist, C.; Kelderman, G.; Morrett, H.; Sinsheimer, R. L.; Elings, V.; Bustamante, C.; Hansma, P. K. *Science* **1992**, 256, 1180–1184.
- (45) Kiriya, A.; Gorodyska, G.; Minko, S.; Jaeger, W.; Stepanek, P.; Stamm, M. *J. Am. Chem. Soc.* **2002**, 124, 13454–13462.
- (46) Grubb, D. T.; Jelinski, L. W. *Macromolecules* **1997**, 30, 2860–2867.
- (47) Sapede, D.; Seydel, T.; Forsyth, V. T.; Koza, M. M.; Schweins, R.; Vollrath, F.; Riekel, C. *Macromolecules* **2005**, 38, 8447–8453.
- (48) Shulha, H.; Foo, C. W. P.; Kaplan, D. L.; Tsukruk, V. V. *Polymer* **2006**, 47, 5821–5830.